ILETA International Information and Engineering Technology Association

International Journal of Heat and Technology

Vol. 43, No. 5, October, 2025, pp. 1869-1876

Journal homepage: http://iieta.org/journals/ijht

Detachable Heat Storage for Nighttime Dehydration in Solar Food Dryers

Check for updates

Reza Abdu Rahman^{1,2}, Sulistyo¹, Mohamad Said Kartono Tony Suryo Utomo¹

- ¹ Department of Mechanical Engineering, Universitas Diponegoro, Semarang 50275, Indonesia
- ² Department of Mechanical Engineering, Faculty of Engineering, Universitas Pancasila, DKI Jakarta 12640, Indonesia

Corresponding Author Email: sulistyo@lecturer.undip.ac.id

Copyright: ©2025 The authors. This article is published by IIETA and is licensed under the CC BY 4.0 license (http://creativecommons.org/licenses/by/4.0/).

https://doi.org/10.18280/ijht.430526

Received: 28 August 2025 Revised: 14 October 2025 Accepted: 25 October 2025 Available online: 31 October 2025

Keywords:

charging, Eucheuma spinosum, humidity, thermal, water content

ABSTRACT

The operation of the solar-powered dehydrator (SPD) works only in daytime as the system relies on solar radiation. It causes certain technical barriers, especially for drying high water content food products. To overcome the challenge, a heat storage apparatus (HSA) is integrated to enhance the operation at nighttime. In this work, we propose a novel concept for integrated HSA-SPD. The HSA employs a multicell arrangement and works in a passive-active system. The proposed model is installed as a separate component, which allows the HSA can be detached during the daytime. Experimental tests are performed by adjusting the discharging period of HSA for two different SPD models: greenhouse (GH) and drying cabinet (DC). The finding shows the nighttime dehydration without using SPD evaporates around 11.6% water content of the products for 10 hours of operation, while GH and DC indicate a higher rate around 16.4% and 21.3%, respectively. Discharging the HSA at the initial dehydration stages leads to a lower evaporation rate with total water removal only 20.7% (GH) and 28.9% (DC), compared to discharging at the second dehydration that leads to a higher water removal up to 26.1% (GH) and 33.8% (DC). It shows detachable HSA offers flexible operation to maximize dehydration rate for SPD in nighttime operation.

1. INTRODUCTION

Transition in the energy sector becomes mandatory as the global population and demand for energy increase tremendously. Various options are introduced to address the challenge, including the attention of power plant sectors [1], enhancing the clean hydrogen process [2], and system energy optimization [3]. Specific attention is focused on thermal processing in the food sector, which accounts for large energy consumption. It is affected by the requirement to process the food in a certain quality and preservation to improve the storage ability of the produced food. For example, the drying process for seaweed allows for improving the quality of the final product, leading to a higher selling price and improving the quality of the seaweed farmer. Unfortunately, the drying process is generally performed using a conventional approach, which reduces the final quality of the product due to dirt exposure and an uncontrolled drying process [4]. Technology intervention is introduced to minimize the issue, particularly for using solar-powered drying (SPD), which has minimal impact on the environment and decreases energy consumption.

A positive trend is shown for the development of SPD technology, particularly for using the greenhouse concept. It accelerates the drying process, reduces the soiling risk, and produces a higher quality of dried product. Modification for the system is relatively simple, including the possibility to combine the system with renewable electric sources like wind turbines and photovoltaic [5-7]. It reduces the total drying

duration and allows a higher ratio to harvest renewable energy for the drying process. From the industrial perspective, the system is combined with a biomass burner by extracting heat from waste combustion. Therefore, adding more energy to the system becomes a crucial aspect to optimize the SPD technology.

The key function for drying bioproducts is the dehydration process. It involves heat and mass transfer, especially for a closed dryer unit. Sharma et al. [8] assessed the operation of indirect drying, which was equipped with an air heater, indicating a better heat utilization for the proposed model around 67%. Singh and Gaur [9] focused on the sustainability assessment for hybrid SPD technology, demonstrating that the combined system with energy addition from external solar utilization leads to faster drying, removing 84.6% of water content from the product within 10 hours. Selimefendigil et al. [10] utilized a passive method for accelerating the drying. The system was equipped with graphene nanoplatelets for the paint decoration within the SPD system, resulting in a double increment of the exergy efficiency compared to the basic SPD system. Despite the improvement, the system still requires modification to ensure its operation during nighttime without the intervention of solar radiation. At this point, the heat storage apparatus (HSA) becomes a reliable option to obtain continuous operation of the SPD system.

The excess solar energy in the daytime is possible to be stored in the HSA. It is achieved by heating the material within the system, which generally uses a solid-liquid transition material [11-14]. The system is developed extensively, including the modification of the storage material [15-17], optimization for the heat exchanger within the system [18], and system integration [19-21]. The apparatus is combined for the SPD system, indicating a suitable drying performance. Rouzegar et al. [22] developed a hybrid SPD with air-charged HSA, showing that the drying capability improved by around 74.06%. Mirzaee et al. [23] evaluated the location of HSA within the SPD system, indicating that certain influence on the drying efficiency can be influenced by the location of the HSA, while a positive outcome remains achieved for the system equipped with HSA. Numerical assessment was performed by Lad et al. [24], focusing on the combined tube collector with HSA, showing that the combined system is preferable to reduce the total drying time of the processed product.

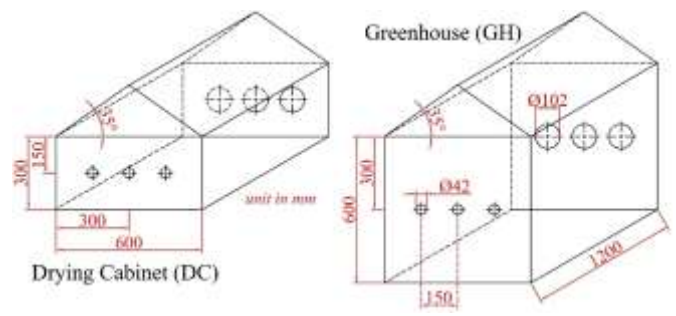
The integration for SPD-HSA comes in various approaches. Chaatouf et al. integrated the system by placing the storage material within a container tube, which was designed according regenerator concept, indicating the drying duration decreased about 33.3% [25]. A straightforward method is employed by combining the HSA and the air heater. The proposed method indicated that the power quality and storage efficiency were affected by the type of storage material, while the general result indicated a better temperature outlet of the integrated air heater with HSA [26]. Numerical optimization was performed for the given model. It showed that the tilt angle of the collector affects the maximum solar absorption and a higher mass flow rate [27]. Integrating the HSA with an air heater results in a simple configuration since the working fluid is air, which can be directly used for supplying hot temperature to the drying chamber [28]. However, direct operation has a significant drawback regarding the flexibility of the operation and the temperature limitation of the HSA since it relies on the surface temperature of the air heater.

Integrating the HSA unit with the air heater reduces the technical storage capability. It is affected by the temperature limitation of HSA, reducing the maximum working temperature of the SPD. Thus, employing direct operation for the HSA is preferable to achieve a higher temperature limit. It also improves the operational aspect since the HSA can be charged by a direct PV system [29] or grid-powered electricity [30]. Previous studies generally focus on the development of the HSA system, which is integrated by a solar air heater, while the operation of the SPD model is analyzed for direct operation during daytime. Further assessment can be taken by evaluating the operation of the integrated SPD-HSA system under nighttime operation.

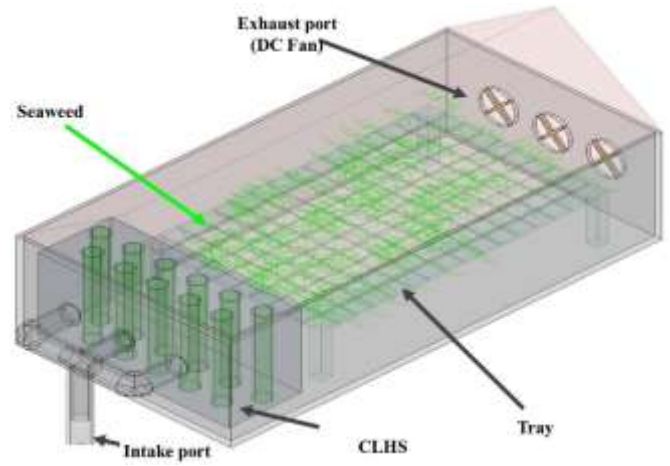
The nighttime drying becomes a new trend as a part of optimization to maximize the drying capacity and reduce the potential of post-harvest loss. Therefore, the goal of this work is to boost the drying process by using detachable HSA. The HSA allows for multi-stage heat release that is expected to improve the nighttime dehydration process. The evaluation is designed to understand the role of HSA for nighttime operation, including the effect of the volumetric drying chamber on the typical SPD model. The case-by-case assessment is expected to provide a detailed analysis to improve the capability of the optimal drying process in the absence of solar radiation, reducing the potential of post-harvest loss and improving the production capacity in a sustainable way for drying food products.

2. MATERIALS AND METHODS

Figure 1(a) shows the dimensions of the SPD for the experimental test. There were two SPD models that were evaluated simultaneously: Greenhouse (GH) and drying cabinet (DC). The developed model was aimed at understanding the effect of the volumetric ratio for drying. Each model has an identical area considering its function for daytime drying, where the variation was taken on the height of each model with a ratio of 1:2. The cladding was made of thin (200 μ m) polyethylene plastic. The HSA was designed as a novel model of clustered latent heat storage (CLHS) using stabilized-palmitic acid as storage material was located within the drying chamber that operates under a passive-active scenario. The detailed performance of the CLHS and properties of the storage material can be read from our previous work [31-33].



(a) Detailed dimensions of SPD



(b) Arrangement of the components of the SPD

Figure 1. Apparatus of the SPD unit

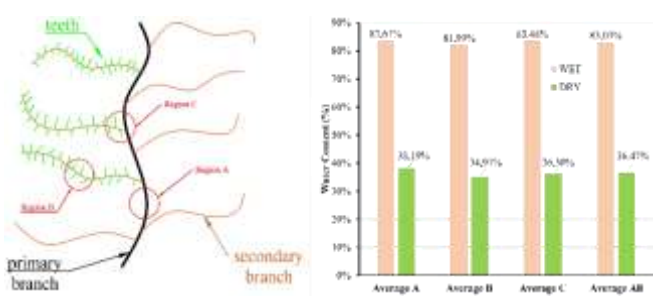
Figure 2(a) shows the photograph of the seaweed (Eucheuma spinosum/E.Sp) as received from the local market. The wet version (Figure 2(a)) has a high-water content, which can be seen clearly in the water absorption by the paper towel (red arrow). There is a significant change in the dried version, which is generally smaller and has a shrinkage characteristic. The water content for each version was measured using a moisture analyzer (Mettler Toledo). The measurement was taken at different regions (Figure 2(b)) to accommodate the variation of water content within the body of the sample. The summary of moisture content is plotted in Figure 2(b).

The experiment was performed simultaneously for the two models (GH and DC). At first, the HSA was charged until reaching 90°C (upper limit of HSA). The fully charged HSA was moved to the inside area of the dehydrator according to

the designed time. There were three exhaust fans (brushless motor fan) with an average power consumption of 2.4 Watts. The drying load (wet seaweed) was 1,000 grams (\pm 20 grams). There were five different cases from this work (Table 1). There were two versions for locating the HSA inside the dehydrator. The first version was located in the HSA after one hour of operation (20:00), which was considered the initial dehydration stage of the product. The second version was 00:00 (five hours after the operation), which was considered the second dehydration stage.



(a) Photograph of wet and dry seaweed



(b) Sampling and water content of the seaweed

Figure 2. Characteristic of dehydration load (seaweed)

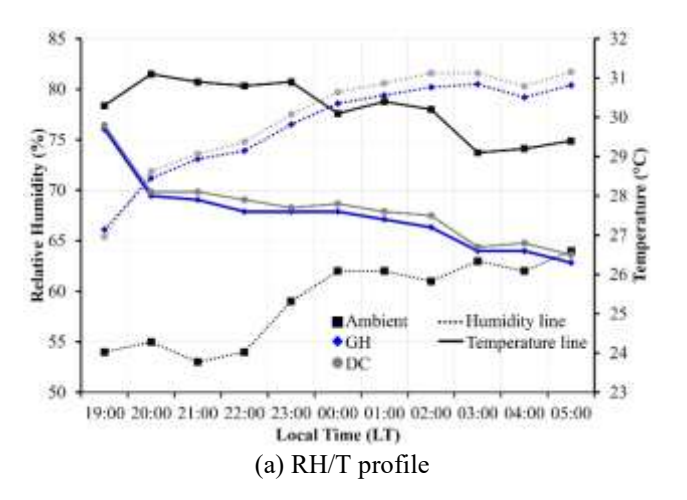
Table 1. Detailed case assessment of integrated SPD-HSA

Case Number	DC	GH	Information
Case 1	✓	✓	
Case 2	✓ + HSA (a)	✓	HSA (a) means the
Case 3	✓	✓ + HSA (a)	stored heat was discharged at 20:00
Case 4	✓ + HSA (b)	✓ HSA (b) mea	HSA (b) means the stored heat was discharged at 00:00
Case 5	✓	✓ + HSA (b)	discharged at 00.00

One critical factor for nighttime assessment is the heat storage utilization (HSU) factor. It indicates the effective energy consumption of dehydration at nighttime. The total energy input is accounted for by charging the HSA, which was obtained as the total electrical input [34] from the charge, and the total energy to operate the suction fan. The useful energy to dehydrate the product is proportional to the latent heat of vaporization of water and total water removal from the product during the dehydration [35]. Thus, specific HSU can be obtained to indicate the effectiveness of the dehydration process at night.

3. RESULTS AND DISCUSSION

The experiment was performed for the designed case (Table 1). The temperature (T) and relative humidity (RH) were measured as critical parameters of the drying process. In addition, the mass of the product was measured to obtain the total water removal from the process. Figure 3(a) shows the measured RH/T for case one. The humidity for the dryer (Figure 3(a)) shows a higher value compared to the ambient. As it result, the temperature inside the unit becomes lower as the water evaporates from the product (Figure 3(a)). Focusing on the dryer type, it seems the DC type has a higher humidity which followed by a lower temperature, compared to the GH type. It confirms the effect of volume within the drying unit. It contributes to a higher degree of evaporation rate, resulting in a better dryness level of the product (Figure 3(b)). In addition, the open drying (OD) has the lowest value since it relies on natural convection without intervention from solar radiation, making the drying rate at nighttime is extremely slow.



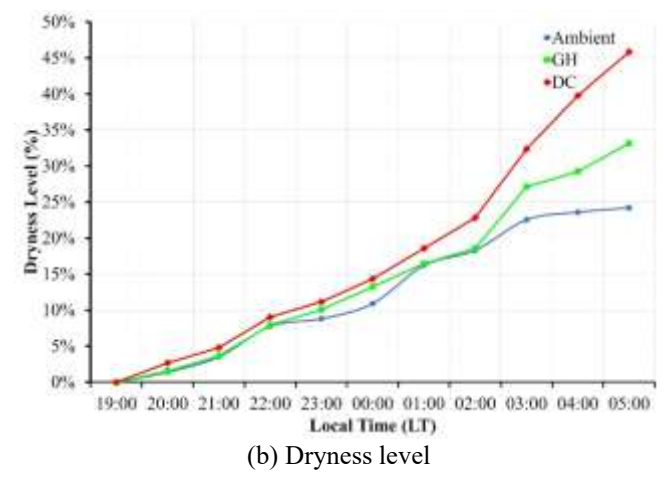


Figure 3. Operational characteristics from the evaluation of case 1

The operation of HSA contributes positively to the nighttime drying. The humidity drops significantly at the initial discharge, causing the lowest humidity can be achieved at 49.4% (Figure 4(a)). It is affected by the increment in temperature inside the dryer (Figure 4(a)), resulting in dryer air being distributed to the product. It allows the dryer to achieve a higher evaporation rate (Figure 4(b)) in the effective discharge stage. The evaporation goes rapidly, confirming that the liberation of water content becomes more effective. However, the maximum duration for the HSA was only 4

hours, making the evaporation become lower once the stored energy is fully discharged.

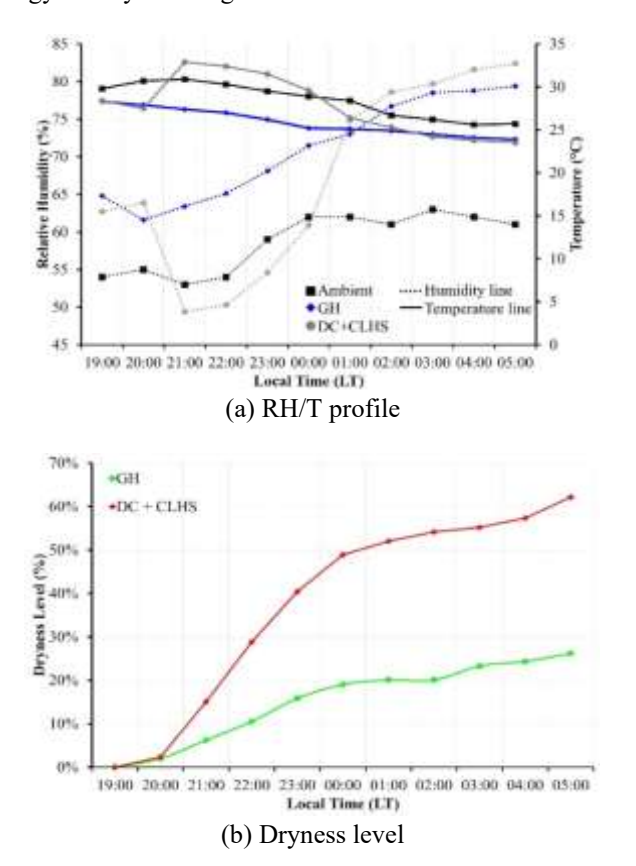


Figure 4. Operational characteristics from the evaluation of case 2

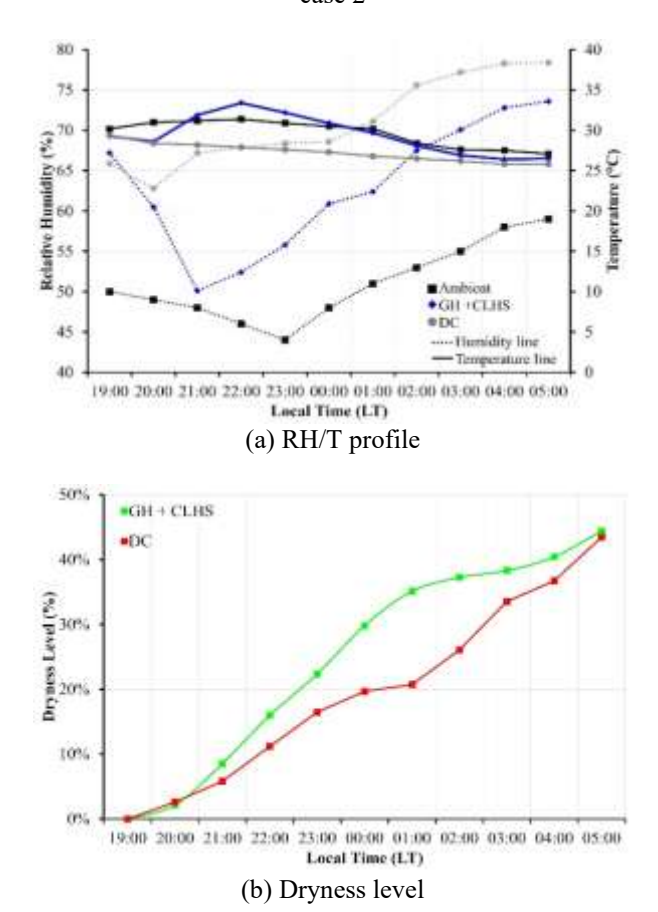


Figure 5. Operational characteristics from the evaluation of case 3

In the case of the GH type, the integration HSA for nighttime drying indicates a positive contribution. Unfortunately, the value is relatively lower in terms of the final dryness level. The decrement in RH level for GH type, along with discharge stage for the HSA (Figure 5(a)), shows the lowest value (50.1%). The highest temperature (Figure 5(a)) is close to the DC type in the second case. However, the increment of water removal for the GH type is 12.6%, much lower than the DC type. As a result, the final dryness level for the GH type with HSA is relatively similar to the DC type without HSA (Figure 5(b)).

The integrated system with HSA shows a notable improvement in the final dryness level. Despite the variation between GH and DC, each model demonstrates a higher final dryness level compared to the non-integrated system. There is one identical phenomenon that can be observed according to the dryness curve. The highest evaporation occurs simultaneously with the heat liberation from HSA and initial water content removal from the product. Since the HSA has a limited discharge duration, it is worth modifying the discharge stage after the product passes the initial failing rate. Thus, we performed two additional cases where the HSA was discharged after five hours drying operation (approximately at 00:00 LT).

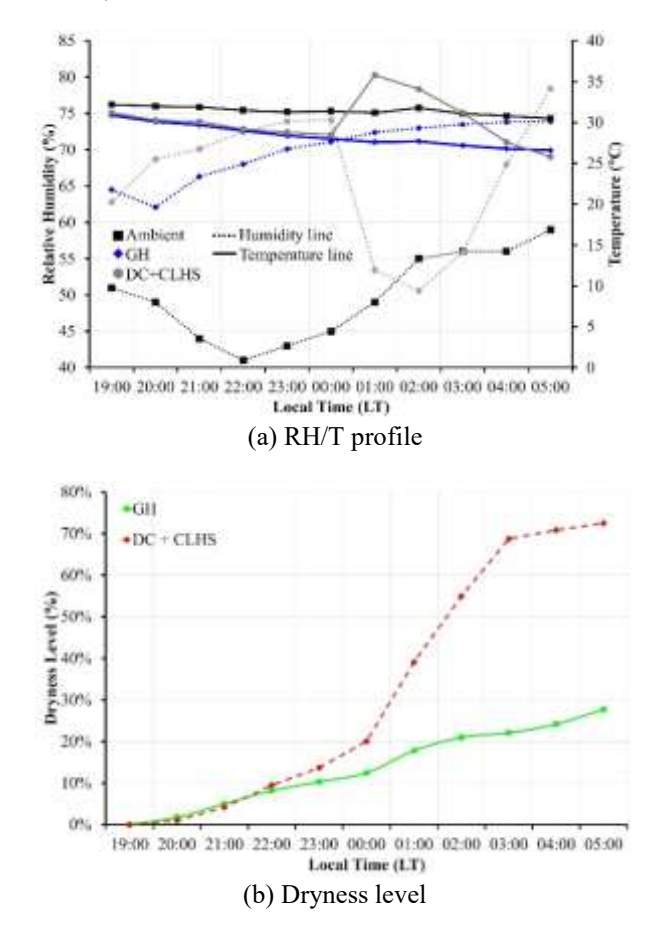
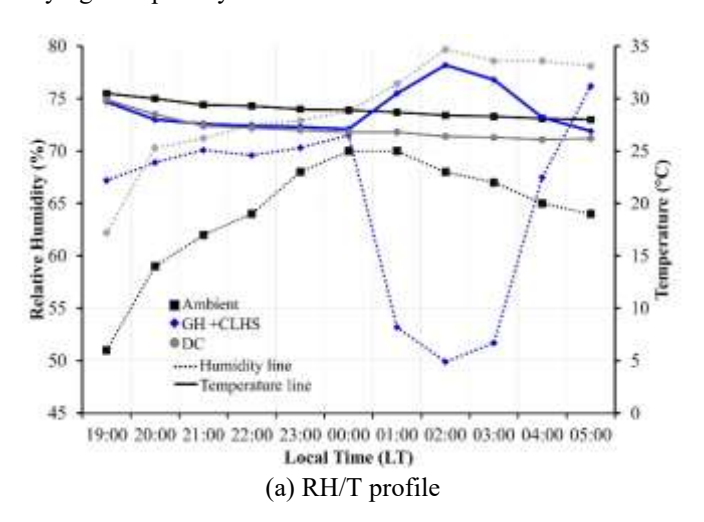


Figure 6. Operational characteristics from the evaluation of case 4

The HSA was discharged at 00:00, and as observed in Figure 6(a), the corresponding humidity and temperature change at the given region. The humidity drops to around 20.7%, which is higher compared to the second case. The same condition is also observed for the temperature, which is able to increase by about 7.3°C. It is advantageous since the weather conditions in this time period are insufficient, making

the discharged heat effective to improve the evaporation process. It can be seen during the initial evaporation rate with an average of 4%/hour (Figure 6(b)). As the heat is discharged after passing the first falling rate, the water inside the seaweed pulls out to the surface. The supplied heat at this moment accelerates the evaporation, resulting in a higher final dryness level of the product (72.5%).

The optimum performance of nighttime drying using HSA is also achieved for the GH configuration. As observed in Figure 7(a), the temperature and humidity level changes as the heat is discharged from the HSA. It results in a significant improvement for the final dryness level (Figure 7(b)) compared to the direct operation at the initial drying process (Figure 5(b)). Unfortunately, the maximum dryness level for the GH configuration remains lower than DC. It confirms the role of effective volumetric ratio, making the designed drying chamber important to ensure a high evaporation rate. Despite that, all model confirms the positive impact of the usage of HSA for nighttime drying. It allows the effective drying process can be performed in the nighttime, resulting in an effective continuous drying operation which significantly reduces the drying duration and eventually increases the total drying load per day.



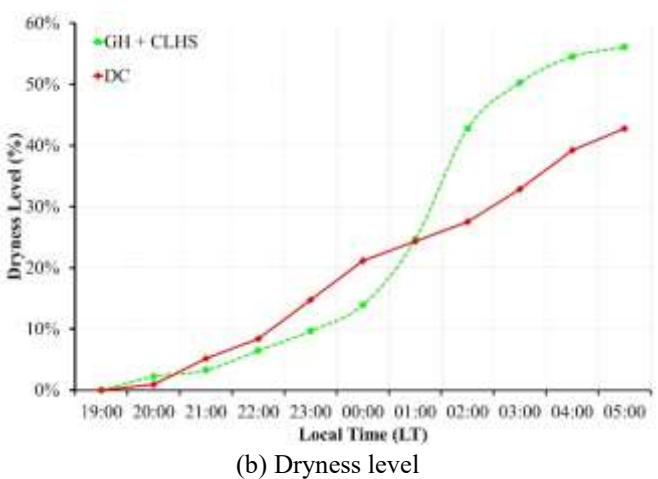


Figure 7. Operational characteristics from the evaluation of case 5

Further discussion is focused on the operational curve of the HSA and overall performance for each case. The temperature profile for the HSA is presented in Figure 8. The charge process using direct heating allows the charging rate can be controlled effectively (200 Watts in this work) to ensure the

heat can be distributed effectively throughout the entire body of solid-liquid transition material (SLTM). It can be observed that the HSM experiences a solid-liquid transition between 54–62°C (green box Figure 8), which is indicated by a lower temperature increment in this region. The next step is the SLTM entering the liquid zone, which starts around 70°C (blue arrow). It is indicated by a rapid temperature increment after passing the solid-liquid transition.

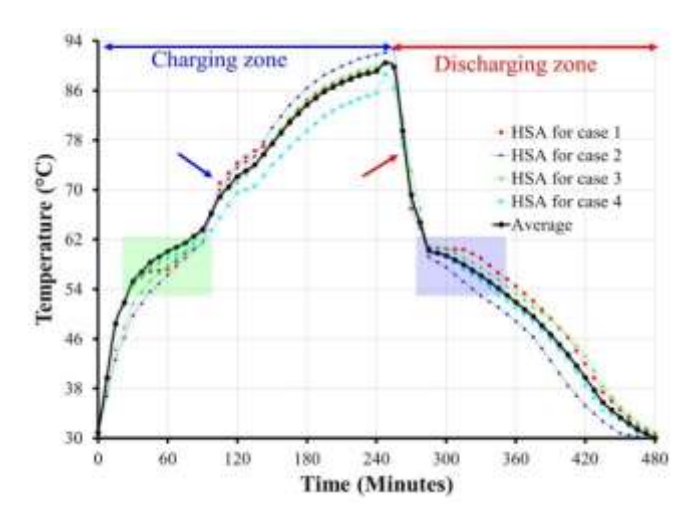


Figure 8. Temperature profile of HSA

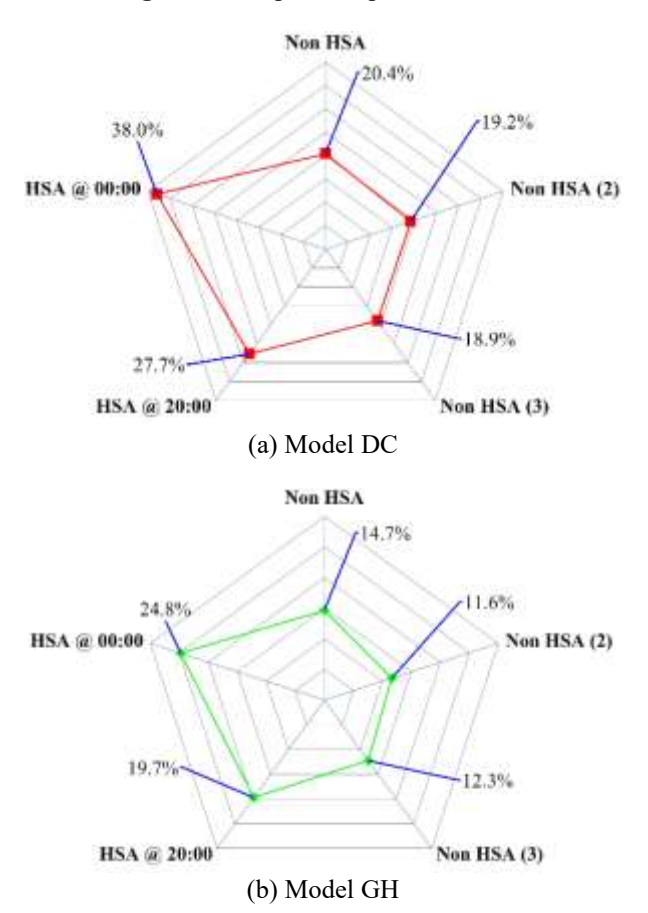


Figure 9. Comparison of heat storage utilization for the dehydration process

The shape-stable effect from the polymer makes the phase change favorable, resulting in a stable melting/freezing process to maximize the heat interaction inside the HSA. The rapid temperature drops at the discharge zone (red arrow in

Figure 8) demonstrate that most of the stored energy at the liquid sensible zone is discharged rapidly to the system. After that, the SLTM enters the solidification region (blue box, Figure 8), indicated by a slow temperature decrease. It contributes to the liquid-solid transition at a relatively identical temperature with the melting transition, showing the SLTM has superior performance with minor supercooling effect [36].

The HSU value is plotted in Figure 9. The optimum size configuration using a smaller unit dehydrator under the same working operation for the DC model (Figure 9(a)) gives the highest HSU value of 38%. This means that 38% of the intake energy for charging the HSA and operating the dehydrator can be used to dehydrate the processed product. Increasing the dehydrator volume for the GH model decreases the HSU factor, obtaining the maximal value at 24.8% (Figure 9(b)). The presented case shows the significant contribution of the proposed model to perform the dehydration process at a higher value using separated HSA, in which the charging process and discharge time can be adjusted according to the requirements and characteristics of the processed product. It also emphasizes that a controllable operation can achieve higher water removal by setting a suitable discharge operation according to the dehydration characteristic of the product.

4. CONCLUSION AND FUTURE OUTLOOK

Improving the nighttime dehydration process of food products using a solar-powered dehydrator (SPD) is achieved by integrating the system with a heat storage apparatus (HSA). The maximum water removal is obtained by 21.3% using the drying cabinet model (DC) for SPD. The HSA is separated from the SPD assembly, making the configuration possible for adjustment to achieve a higher dehydration rate. For example, operating the HSA at the initial dehydration stage only results in 28.9% of water removal using the same SPD. The water removal can be maximized by detaching the HSA from SPD and operating it at the second dehydration stage. As a result, the maximum water removal improves to 33.8%. From an energy perspective, the operation of HSA at the second dehydration stage also reaches the highest heat storage utilization (HSU) by 38%. Therefore, flexible operation with a detachable HSA for SPD significantly boosts the dehydration process and potentially maximizes the energy utilization for drying.

The proposed integration may bring positive benefits as the system is able to operate at nighttime, potentially shortening the total duration of the drying process and preventing product deterioration due to the absence of heat at night. However, the present work is limited by operating the HSA with a specific type of material and identical weather conditions. Thus, we suggest the following topics for future improvement:

- Evaluation of the long-term stability of HSA material and potential modification to improve the total storage capacity, as well as system control.
- Evaluation under different weather conditions, particularly
 for full cycle operation (day and night), to evaluate the
 effectiveness of the process and obtain detailed practical
 applicability for the drying process, including the
 evaluation using different food products or drying loads.
- Detailed techno-economic assessment for the system to address the potential of commercialization for the proposed model.

Addressing the aforementioned topics consequently leads to

a higher technology level and real-world system for the possible implementation of integrated HSA-SPD to support the transition in renewable thermal energy systems and sustainable food processing.

ACKNOWLEDGMENT

The study is supported by the Ministry of Research, Technology, and Higher Education of Indonesia under *Penelitian Disertasi Doktor* (Grant No.: 601-12/UN7.D2/PP/VI/2024).

REFERENCES

- [1] Anggara, F., Ayu Besari, D.A., Timotius, D., Amijaya, D.H., Al Hasunah, W., Andriani, A., Murti Petrus, H.T.B., Dhewangga Putra, R.D., Fahrialam, A. (2024). Understanding FABA composition in coal-fired power plants: Impact of operating conditions and combustion efficiency on ash characteristics A case study in PT Bukit Asam, South Sumatra, Indonesia. Results in Engineering, 23: 102590. https://doi.org/10.1016/j.rineng.2024.102590
- [2] Putra, R.D.D., Wijaya, Y.P., Smith, K.J., Trajano, H.L., Kim, C.S. (2022). Lignin depolymerization and monomeric evolution during fast pyrolysis oil upgrading with hydrogen from glycerol aqueous phase reforming. Fuel, 324: 124556. https://doi.org/10.1016/j.fuel.2022.124556
- [3] Mehrjardi, S.A.A., Khademi, A., Safavi, S.M.M. (2025). Machine learning approach to balance heat transfer and pressure loss in a dimpled tube: Generative adversarial networks in computational fluid dynamics. Thermal Science and Engineering Progress, 57: 103116. https://doi.org/10.1016/j.tsep.2024.103116
- [4] Langford, A., Zhang, J., Waldron, S., Julianto, B., Siradjuddin, I., Neish, I., Nuryartono, N. (2022). Price analysis of the Indonesian carrageenan seaweed industry. Aquaculture, 550: 737828. https://doi.org/10.1016/j.aquaculture.2021.737828
- [5] Atalay, H., Yavaş, N., Turhan Çoban, M. (2022). Sustainability and performance analysis of a solar and wind energy assisted hybrid dryer. Renewable Energy, 187: 1173-1183. https://doi.org/10.1016/j.renene.2022.02.020
- [6] Ismail, Pane, E.A., Rahman, R.A. (2022). An open design for a low-cost open-loop subsonic wind tunnel for aerodynamic measurement and characterization. HardwareX, 12: e00352. https://doi.org/10.1016/j.ohx.2022.e00352
- [7] Sehrawat, R., Sahdev, R.K., Chhabra, D., Tiwari, S. (2023). Experimentation and optimization of phase change material integrated passive bifacial photovoltaic thermal greenhouse dryer. Solar Energy, 257: 45-57. https://doi.org/10.1016/j.solener.2023.04.024
- [8] Sharma, M., Atheaya, D., Kumar, A. (2023). Performance evaluation of indirect type domestic hybrid solar dryer for tomato drying: Thermal, embodied, economical and quality analysis. Thermal Science and Engineering Progress, 42: 101882. https://doi.org/10.1016/j.tsep.2023.101882
- [9] Singh, P., Gaur, M.K. (2021). Sustainability assessment of hybrid active greenhouse solar dryer integrated with

- evacuated solar collector. Current Research in Food Science, 4: 684-691. https://doi.org/10.1016/j.crfs.2021.09.011
- [10] Selimefendigil, F., Şirin, C., Öztop, H.F. (2022). Improving the performance of an active greenhouse dryer by integrating a solar absorber north wall coated with graphene nanoplatelet-embedded black paint. Solar Energy, 231: 140-148. https://doi.org/10.1016/j.solener.2021.10.082
- [11] Khademi, A., Darbandi, M., Behshad Shafii, M., Schneider, G.E. (2019). Numerical simulation of thermal energy storage process benefiting from the phase change materials concept. AIAA Propulsion and Energy Forum and Exposition, 2019: 1-9. https://doi.org/10.2514/6.2019-4225
- [12] Rahman, R.A., Setiawan, D., Nugroho, A., Putra, R.D.D. (2025). Employing sugar alcohol-based phase change material for integrated compact thermal battery (ICTB): Experimental exploration for future configuration of modern space heating with thermal storage. Applied Thermal Engineering, 271: 126317. https://doi.org/10.1016/j.applthermaleng.2025.126317
- [13] Khademi, A., Darbandi, M., Schneider, G.E. (2020). Numerical study to optimize the melting process of phase change material coupled with extra fluid. AIAA Scitech 2020 Forum, 1 PartF: 1-6. https://doi.org/10.2514/6.2020-1932
- [14] Firman, L.O.M., Rahmalina, D., Ismail, Rahman, R.A. (2023). Hybrid energy-temperature method (HETM): A low-cost apparatus and reliable method for estimating the thermal capacity of solid liquid phase change material for heat storage system. HardwareX, 16: e00496. https://doi.org/10.1016/j.ohx.2023.e00496
- [15] Bian, Z., Hou, F., Chen, J.Q., Wang, H. (2024). Numerical analysis on the effect of graded porosity in closed-cell metal foams/PCM composites. Case Studies in Thermal Engineering, 55: 104145. https://doi.org/10.1016/j.csite.2024.104145
- [16] Khademi, A., Favakeh, A., Darbandi, M., Shafii, M.B. (2019). Numerical and experimental study of phase change material melting process in an intermediate fluid. In 7th International Conference on Energy Research and Development, pp. 16-23.
- [17] Favakeh, A., Khademi, A., Shafii, M.B. (2019). Experimental study of double solid phase change material in a cavity. In 7th International Conference on Energy Research and Development, pp. 24-31.
- [18] Mehrjardi, S.A.A., Khademi, A., Fazli, M. (2024). Optimization of a thermal energy storage system enhanced with fins using generative adversarial networks method. Thermal Science and Engineering Progress, 49: 102471. https://doi.org/10.1016/j.tsep.2024.102471
- [19] Alqsair, U.F., Abdullah, A.S., Younes, M.M., Omara, Z.M., Essa, F.A. (2024). Augmenting hemispherical solar still performance: A multifaceted approach with reflectors, external condenser, advanced wick materials, and nano-PCM integration. Case Studies in Thermal Engineering, 61: 104890. https://doi.org/10.1016/j.csite.2024.104890
- [20] Khademi, A., Mehrjardi, S.A.A., Tiari, S., Mazaheri, K., Shafii, M.B. (2022). Thermal efficiency improvement of brayton cycle in the presence of phase change material. In Proceedings of the 9th International Conference on Fluid Flow, Heat and Mass Transfer (FFHMT'22),

- Niagara Falls, Canada, pp. 1-9. https://doi.org/10.11159/ffhmt22.135
- [21] Fazli, M., Mehrjardi, S.A.A., Mahmoudi, A., Khademi, A., Amini, M. (2024). Advancements in pulsating heat pipes: Exploring channel geometry and characteristics for enhanced thermal performance. International Journal of Thermofluids, 22: 100644. https://doi.org/10.1016/j.ijft.2024.100644
- [22] Rouzegar, M.R., Abbaspour-Fard, M.H., Hedayatizadeh, M. (2023). Design, thermal simulation and experimental study of a hybrid solar dryer with heat storage capability. Solar Energy, 258: 232-243. https://doi.org/10.1016/j.solener.2023.05.003
- [23] Mirzaee, P., Salami, P., Akhijahani, H.S., Zareei, S. (2023). Life cycle assessment, energy and exergy analysis in an indirect cabinet solar dryer equipped with phase change materials. Journal of Energy Storage, 61: 106760. https://doi.org/10.1016/j.est.2023.106760
- [24] Lad, P., Kumar, R., Saxena, R., Patel, J. (2023). Numerical investigation of phase change material assisted indirect solar dryer for food quality preservation. International Journal of Thermofluids, 18: 100305. https://doi.org/10.1016/j.ijft.2023.100305
- [25] Chaatouf, D., Raillani, B., Salhi, M., Amraqui, S., Mezrhab, A. (2023). Experimental and numerical study of a natural convection indirect solar dryer with PCM tubes: Dynamic, thermal and nutritional quality analysis. Solar Energy, 264: 111975. https://doi.org/10.1016/j.solener.2023.111975
- [26] Brahma, B., Shukla, A.K., Baruah, D.C. (2023). Design and performance analysis of solar air heater with phase change materials. Journal of Energy Storage, 61: 106809. https://doi.org/10.1016/j.est.2023.106809
- [27] Chaatouf, D., Ghiaus, A.G., Amraqui, S. (2022). Optimization of a solar air heater using a phase change material for drying applications. Journal of Energy Storage, 55: 105513. https://doi.org/10.1016/j.est.2022.105513
- [28] Ghritlahre, H.K., Verma, M., Parihar, J.S., Mondloe, D.S., Agrawal, S. (2022). A detailed review of various types of solar air heaters performance. Solar Energy, 237: 173-195. https://doi.org/10.1016/j.solener.2022.03.042
- [29] Rahman, R.A., Sulistyo, S., Utomo, M.S.K.T.S., Ragil, D., Suyitno, B.M. (2024). Experimental evaluation on the power characteristic of direct-photovoltaic charging for thermal storage equipment. Mechanical Engineering for Society and Industry, 4(1): 115-122. https://doi.org/10.31603/mesi.11493
- [30] Szajding, A., Kuta, M., Cebo-Rudnicka, A., Rywotycki, M. (2023). Analysis of work of a thermal energy storage with a phase change material (PCM) charged with electric heaters from a photovoltaic installation. International Communications in Heat and Mass Transfer, 140: 106547. https://doi.org/10.1016/j.icheatmasstransfer.2022.10654
- [31] Rahman, R.A., Sulistyo, Utomo, M.S.K.T.S., Hutomo, M.B.P., Firman, L.O.M. (2024). Performance evaluation of enhanced clustered latent heat system for air heater using modified organic material. International Journal of Thermofluids, 23: 100807. https://doi.org/10.1016/j.ijft.2024.100807
- [32] Rahman, R.A., Sulistyo, Utomo, M.S.K.T.S., Putra, R.D.D. (2024). The optional approach in recycling

- plastic waste for energy storage application: A detailed evaluation of stabilized–hexadecanoic acid/plastic. Case Studies in Chemical and Environmental Engineering, 9: 100751. https://doi.org/10.1016/j.cscee.2024.100751
- [33] Yuseva, D.S., Anggrainy, R., Putra, R.D.D., Rahman, R.A. (2024). Performance evaluation of combined passive/active thermal charge/discharge latent heat tank with stabilized-solid-liquid storage material for intermediate thermal storage system. International Journal of Thermofluids, 23: 100732. https://doi.org/10.1016/j.ijft.2024.100732
- [34] Waluyo, J., Putra, R.D.D., Adhitya, D.C., Rahman, R.A. (2025). Parametric operational analysis of hybrid thermo-electric/fluid-active thermal storage for domestic

- water heating system. Solar Energy Materials and Solar Cells, 286: 113575. https://doi.org/10.1016/j.solmat.2025.113575
- [35] Embiale, D.T., Gunjo, D.G. (2023). Investigation on solar drying system with double pass solar air heater coupled with paraffin wax based latent heat storage: Experimental and numerical study. Results in Engineering, 20: 101561. https://doi.org/10.1016/j.rineng.2023.101561
- [36] Shamseddine, I., Pennec, F., Biwole, P., Fardoun, F. (2022). Supercooling of phase change materials: A review. Renewable and Sustainable Energy Reviews, 158: 112172. https://doi.org/10.1016/j.rser.2022.112172